



Science Arts & Métiers (SAM)

is an open access repository that collects the work of Arts et Métiers ParisTech researchers and makes it freely available over the web where possible.

This is an author-deposited version published in: <https://sam.ensam.eu>
Handle ID: <http://hdl.handle.net/10985/7254>

To cite this version :

Annie-Claude BAYEUL-LAINE, Sophie SIMONET, Gérard BOIS - VAWT with controlled blades : influence of wake of one turbine on power coefficient on the next turbine - In: 5th IC-EpsMsO, Greece, 2013-07-03 - 5th IC-EpsMsO - 2013

Any correspondence concerning this service should be sent to the repository

Administrator : archiveouverte@ensam.eu



VAWT WITH CONTROLLED BLADES: INFLUENCE OF WAKE OF ONE TURBINE ON POWER COEFFICIENT ON THE NEXT TURBINE

Bayeul-Lainé Annie-Claude^{1,*}, Simonet Sophie^{2,*}, Bois Gérard^{3,*}

¹annie-claude.bayeul-laine@ensam.eu

²Sophie.simonet@ensam.eu

³Gerard.bois@ensam.eu

* Arts et Métiers PARISTECH, LML, UMR CNRS 8107, Bd Paul Langevin, 59655 VILLENEUVE D'ASCQ

Keywords: Numerical simulation, unsteady calculations, VAWT, vertical axis, wind turbine, wind turbine arrays

Abstract. Power production from wind turbines is affected by several conditions like wind speed, turbine speed, turbine design, turbulence, changes of wind direction, wake of previous turbines. These conditions are not always optimal and have negative effects on most turbines. The present wind turbine is a small one which allows to be used on roofs or in gardens to light small areas like publicity boards, parkings, roads or for water pumping, heating... This turbine is less affected by these conditions because the blades combine a rotating movement around each own axis and around the main turbine's one. Due to this combination of movements, flow around this turbine is more optimized than classical Darrieus turbines. It has been shown in previous studies that the best configuration was obtained with straight blades, a blade stagger angle comprised between 0 and 8 degrees and a range of non-dimensional velocity from 0.4 to 0.6 for a very good power coefficient of about 0.4 in case of one VAWT. The present study points up the influence of the position of each VAWT in a group of three turbines and of the distances between turbines. It deals on global and local performances of these turbines.

NOMENCLATURE

C_p	Power coefficient		(no units)
C_{eff}	Real torque		(mN/m)
d	Cross wind direction spacing between two turbine zones		(m)
d'	Downwind direction spacing between two turbine zones		(m)
D	Diameter of turbine zone		(m)
L	Length of blade		(m)
M_{ti}	Torque of blade i by turbine axis,		(mN/m)
P_{eff}	Real power		(W)
R	Radius of axis of blades		(=0.62 m)
R_e	Reynolds number based on length of blade	$R_e = \frac{V_0 L}{\nu}$	(no units)
S	Captured swept area		(m ²)
V_0	Wind velocity		(=8 m/s)
WPD	Wind power density	$WPD=4 \cdot P_{eff} / \pi d^2$	(no units)
Z	Number of blades		(Z=3)
α	Blade stagger angle		(degrees)
λ	Blade or tip blade speed ratio	$\lambda = \frac{\omega R_t}{V_0}$	(no units)
ρ	Density of air		(kg/m ³)
θ	Azimuth angle of blade 1		(degrees)
ω_1	Angular velocity of turbine		(rad/s)
ω_2	Angular velocity of pales	$\omega_2 = -\omega_1 / 2$	(rad/s)

1 INTRODUCTION

All wind turbines can be classified in two great families (Leconte et al. ^[9] Martin ^[10]) (i) horizontal-axis wind turbine (HAWTs) and (ii) vertical-axis wind turbine (VAWTs). VAWTs work at low speed ratios. A lot of works was published on VAWTs like Savonius or Darrieus rotors ^[8], Pawsey ^[12]... but few works were published on VAWTs with relative rotating blades (Bayeul-Lainé et al. ^[2, 3], Cooper ^[4, 5], Dieudonné ^[7]) Some inventors discovered this kind of turbine in the same time on different places (Cooper and Dieudonné for example) and made studies these last fifteen years on this kind of VAWTs.

The present study concerns this kind of VAWT technology in which each blade combines a rotating movement around its own axis and a rotating movement around turbine's axis. The blade sketch needs to have two symmetrical planes because the leading edge becomes the trailing edge when each blade rotates once time around the turbine's axis.

In previous studies (Bayeul-Lainé et al., ^[2, 3]) the benefit of rotating elliptic and straight blades was shown: the performance of this kind of turbine was very good and better than those of classical VAWTs for some specific initial blade stagger angles between 0 and 15 degrees. It was shown that each blade's behaviour has less influence on flow stream around next blade and on power performance.

The low influence of Reynolds number on mean power coefficients was also confirmed for different initial blade stagger angles for straight blades. It has only been observed a small increase of mean power coefficient with Reynolds number.

Finally figure 1 gives mean power coefficients for all test cases, for elliptic (EB) and straight blades (SB). The maximum mean numerical coefficient is about 38% for straight blades.

This figure allows summarizing the most important results:

- Bad influence of straight blades comparatively to elliptic blades for an initial blade stagger angle α of 15 degrees
- Better influence of straight blades comparatively to elliptic blades for an initial blade stagger angle of 0 degree and 8 degrees. Maximum mean power coefficient is better for straight.

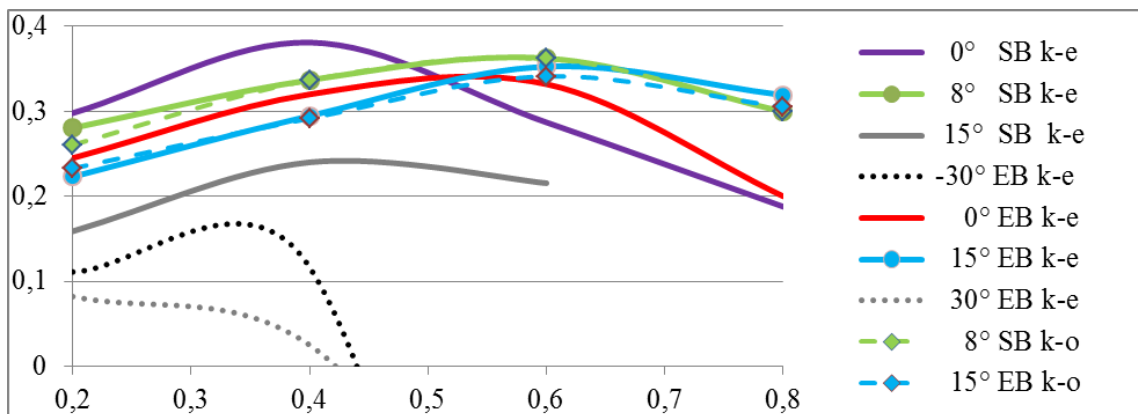


Figure 1. Mean power coefficients for all test cases with blade speed ratios λ
(SB=straight blades, EB=elliptic blades)

The present study points up the influence of adjacent turbine wakes. This aerodynamic constraint limits the amount of power that can be extracted from a given wind farm.

Dabiri ^[6] showed that to maintain 90% of the performance of an isolated HAWT, the turbine in a HAWT farm must be spaced 3-5 turbine diameters apart in the cross wind direction and 6-10 diameters apart in the downwind direction. The power density of such wind farms, defined as the power extracted per unit land area, is 2 and 3 Wm^{-2} as can be seen in Figure 2.

VAWT, whose air foil blades rotate around a vertical axis, have the potential to achieve higher power densities than HAWTs. This possibility arises in part because the swept area of a VAWT rotor need not be equally apportioned between its breadth and its height. By contrast, the circular sweep of HAWT blades dictates that the breadth and height of the rotor swept area are identical. Therefore, whereas increasing HAWT rotor swept area necessarily increases the turbine footprint, it is possible to increase the swept area of a VAWT independent of its footprint, by increasing the rotor blade height. The power density of the VAWT design is more than three times that of the HAWTs, suggesting that VAWTs may be a more effective starting point than HAWTs for the design of wind farms with high power density.

By accommodating a larger number of VAWTs within a given wind farm footprint, Dabiri demonstrated that the power density of the wind farm is increased (blue curve, 30 W m^{-2} wind farm power density). Furthermore, the use of smaller turbines can reduce the complexity and cost of the individual wind turbines, since the smaller wind turbines do not experience the high gravitational, centrifugal, and wind loading that must be withstood by large HAWTs. The less severe design requirements can enable the implementation of less expensive materials and manufacturing processes.

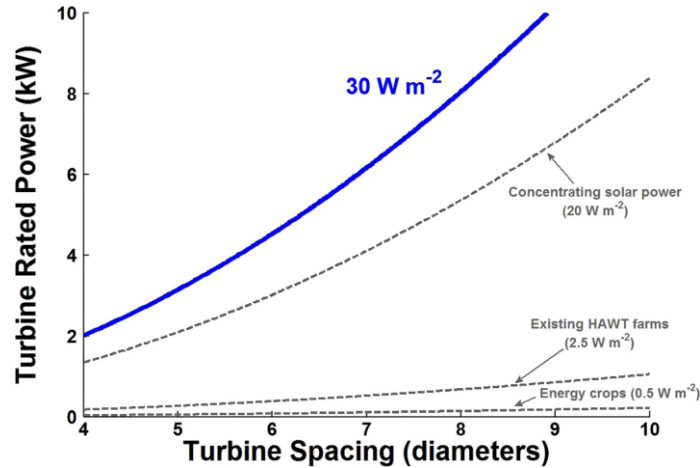


Figure 2. Turbine rated power and spacing combinations for order-of-magnitude increase in wind farm power density relative to existing HAWT farms (Dabiri [6])

2 GEOMETRY AND TEST CASES

Calculations were conducted in case of three VAWTs configuration.

The sketch of the industrial product is shown in Figure 2. Blades have straight sketches, relatively height, so a 2D model was chosen. The calculation domain around turbines is large enough to avoid perturbations as showing in Figure 4. Straight blades are 1050 mm length, each turbine zones has a diameter D equal to 2.4 m. The blade stagger angle α is equal to 8 degrees.

The three VAWT configuration model contains three turbines as can be seen in figures 4 and 5. Details of each turbine zone are shown in figure 7 in which blade zones and turbine zone can be observed. The model contains thirteen zones: outside zone of turbines, three blades zones and zone between outside zone and blades zones named turbine zone for each turbine. Turbine zone has a diameter named D ($D=2,4 \text{ m}$) which includes all blade zones and takes account of a little gap allowing grid mesh to slide. Except outside zone, all other zones have relatively movements. Four interfaces between zones were created for each turbine: an interface zone between outside and turbine zone and an interface between each blade and turbine zone. Details of zones are given in Figures 4 to 7.

The mesh (Figures 6, 7) was refined near interfaces. Prism layer thickness was used around blades. A target size of cells of 0,2 m in the outside zone was used. A minimum size of 2 mm was given near blades. The resulting computational grid is an unstructured triangular grid of number of cells comprised between 300 000 and 600 000 cells.

Unsteady calculations were performed. The angular velocity of turbine is supposed constant and all calculations were realized with $\lambda=0.6$. The time step corresponds to a rotation of 1 degree. So a new mesh was calculated at each time step. The number of revolutions depends on the case calculated and on the stability of the calculation: 10 to 20.

Boundary conditions are velocity inlet to simulate a wind velocity in the lower line of the model ($R_e=560 \text{ 000}$), symmetry planes for right and left lines of the domain and pressure outlet for the upper line of the domain.

Calculations were done with the SST $k-\omega$ Model in which the problem of sensitivity to free-stream/inlet conditions was addressed by Menter [11] who suggested using a blending function (which includes functions of wall distance) that would include the cross-diffusion term far from walls, but not near the wall. This approach effectively blends a $k-\varepsilon$ model in the far-field with a $k-\omega$ model near the wall. Menter also introduced a modification to the linear constitutive equation and dubbed the model containing the SST (shear-stress transport) $k-\omega$ model.

Two kinds of three VAWT configurations were studied: triangular and linear downwind configuration. Indeed, first studies have shown that the turbine wake is very small and localized in the downstream of the wind, so it seems interesting to examine these configurations. The schedule of turbine positions is listed in table 1.

Cases	configurations	d/D	d'/D
T3-3	triangular	1.25	1.25
T3.6-3.6	triangular	1.50	1.50
T4.2-4.2	triangular	1.75	1.75
T6-6	triangular	2.50	2.50
T6-36	triangular	2.50	15.00
L0-6	linear	0.0	2.50
L0-12	linear	0.0	5.00
L0-36	linear	0.0	15.00

Table 1 Schedule of turbine positions



Figure 3. Sketch of the VAWT studied

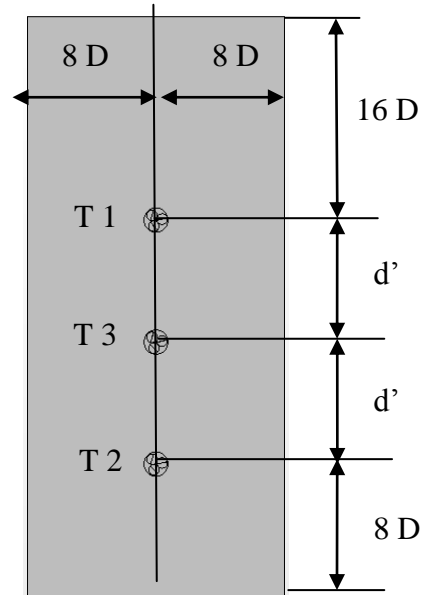


Figure 4. Three VAWT configuration in linear positions

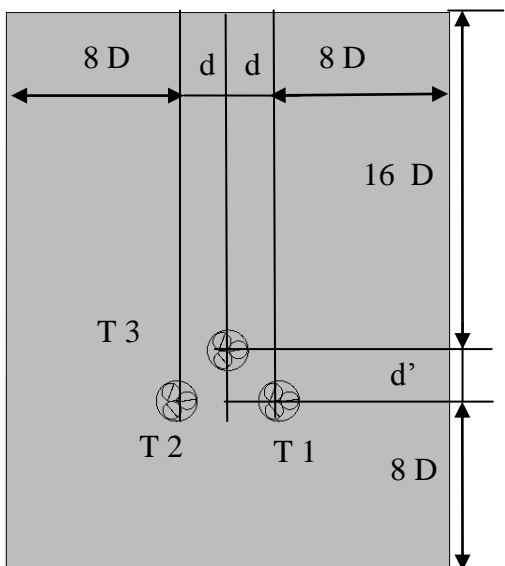


Figure 5. Three VAWT configuration in triangular positions

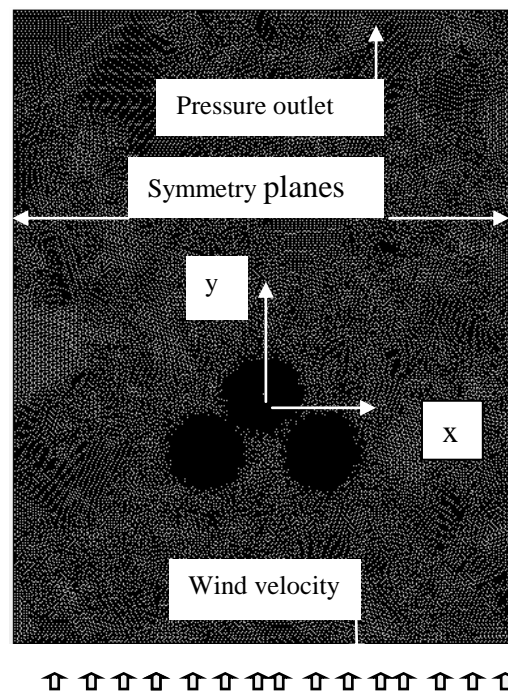


Figure 6. Mesh and boundaries conditions for a three VAWT configuration (triangular positions)

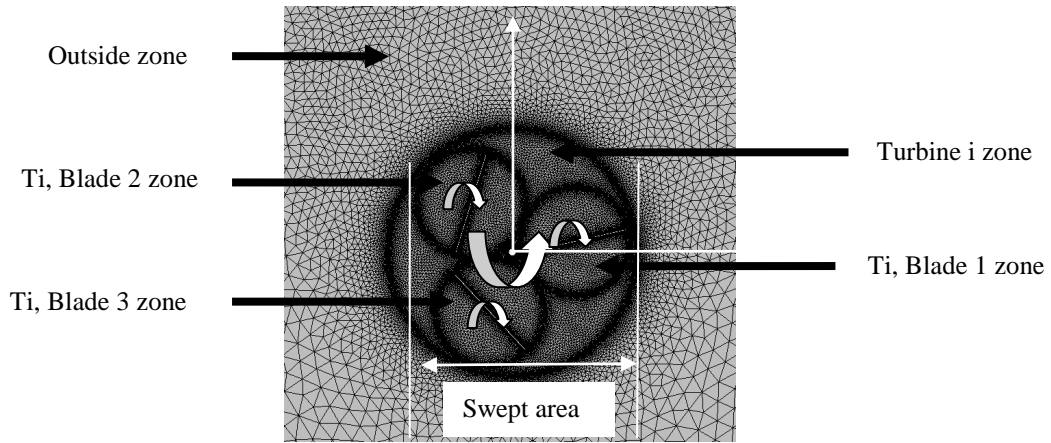


Figure 7. Straight blades : zoom of the mesh of a turbine zone of the VAWT studied

3 TORQUE AND POWER COEFFICIENTS

For this kind of turbine each blade needs energy to rotate around its own axe so real power captured by the turbine has to be corrected.

Code gives torque M_i around turbine axis for each blade, pressure forces and viscosity forces.

$$M_{ii} = \underbrace{\iint_{S_{bladei}} O\vec{G}_i \wedge d\vec{f}}_{C_{1i}} + \underbrace{\iint_{S_{bladei}} G_i\vec{M} \wedge d\vec{f}}_{C_{2i}} = C_{1i} + C_{2i} \quad (1)$$

O is the turbine centre, G_i is the axis centre of blade i and $d\vec{f}$ is elementary force on the blade i due to pressure and viscosity, so

Real power was given by:

$$P_{eff} = \sum_{i=1,2,3} M_{ii} \omega_1 + \sum_{i=1,2,3} C_{2i} \omega_2 = \sum_{i=1,2,3} (M_{ii} + C_{1i}) \frac{\omega_1}{2} \quad (2)$$

with ω_1 , angular velocity of turbine and ω_2 relative angular velocity of each blade around its own axis. And power coefficient is given by equation (3) in which swept area is those showed in figure 5 for the cases with three rotating blades

$$C_p = \frac{P_{eff}}{\frac{\rho S V_0^3}{2}} \quad (3)$$

4 RESULTS

The power coefficient obtained for triangular configurations $T_{i,j}$ and for each turbine T_1 , T_2 and T_3 is plotted in figure 8. The power coefficient of the turbine T_3 , which is downwind of the turbines T_1 and T_2 , is the higher as it can be seen in figures 8 and 9. Moreover the power coefficient for all turbines increases when spacing turbine distance decreases which is really unexpected. These results can be explained by the fact that turbines T_1 and T_3 create a venturi effect at the upwind direction of turbine T_3 . Indeed, the examination of figure 10 shows an increase of velocity at the inlet of turbine 3. The gradients of velocity increase with the decreasing of spacing turbine distance.

So, the calculations for triangular configurations point out that the power developed by a three turbine configurations is greater than those developed by three individual turbines. Moreover these calculations demonstrated that a reasonable spacing distance is $1,25 \cdot D$.

The examination of turbines' wakes (figure 11-12) leads to wonder what is about results for configurations of

turbines in downwind.

The power coefficient obtained for the case T6-36 (figure 13) shows that the venturi effect and that the set effect disappeared. The mean power coefficient of all turbines is about 0.37.

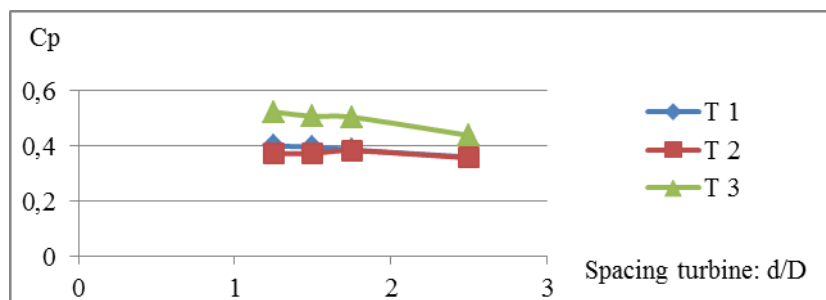


Figure 8. Power coefficient with spacing turbine for cases $T_{i,i}$

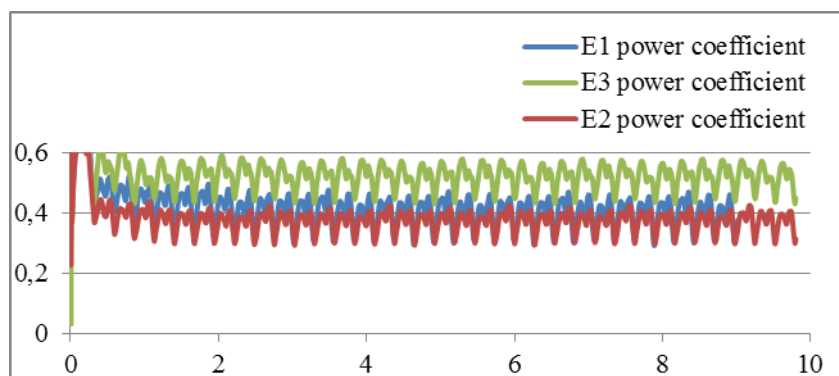


Figure 9. power coefficient with time – case T6-6

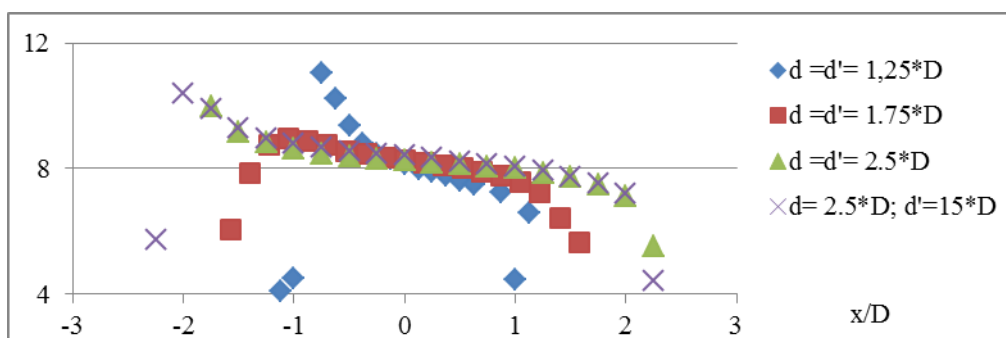


Figure 10. velocity magnitude with non-dimensional x-axis between the center of turbines T1 and T2

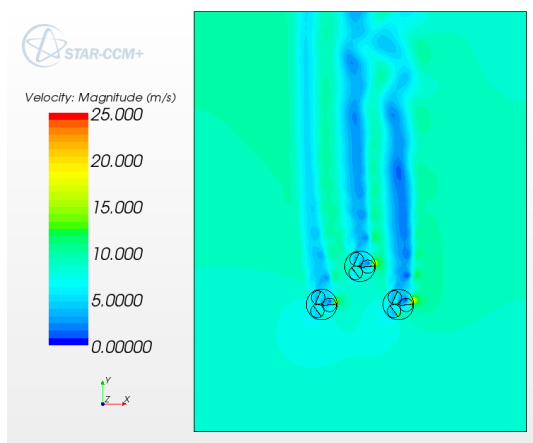


Figure 11. Wakes of turbines, $d=d'=1.25*D$

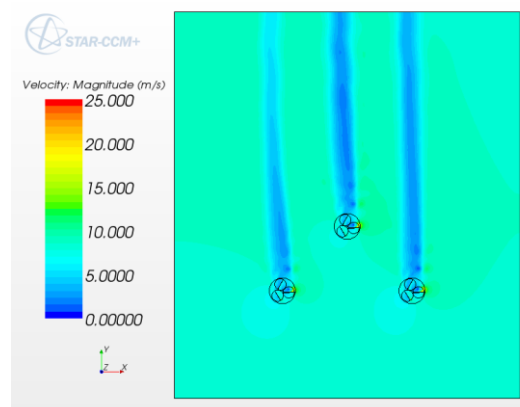


Figure 12. Wakes of turbines, $d=d'=2.50*D$

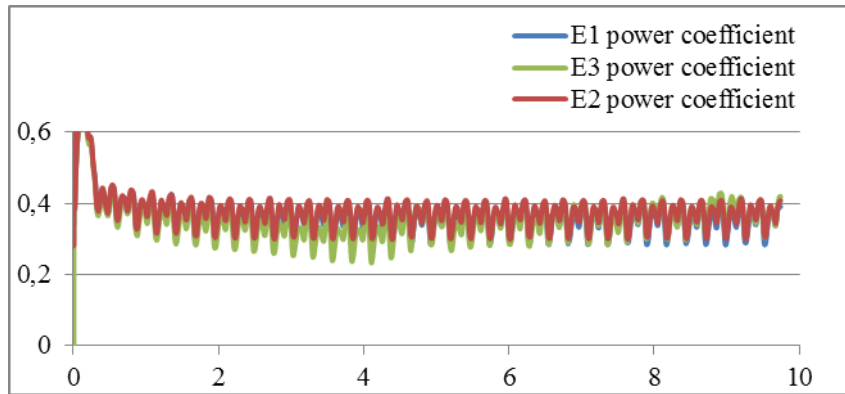


Figure 13. power coefficient with time – case T6-36

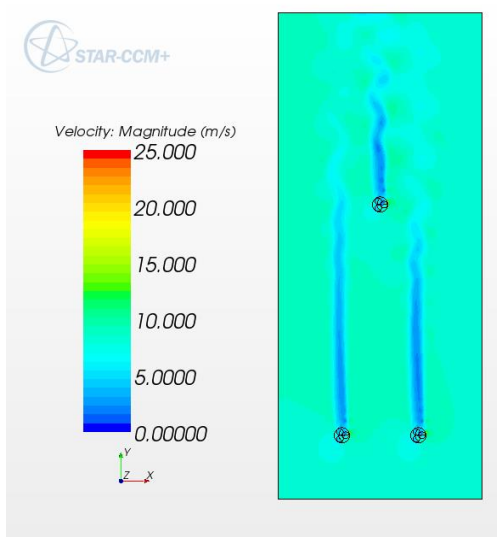


Figure 14. Wakes of turbines, $d=2.50*D$, $d'=15*D$

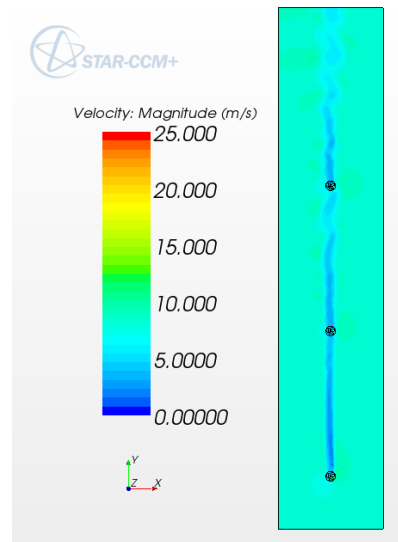


Figure 15. Wakes of turbines, $d'=15*D$

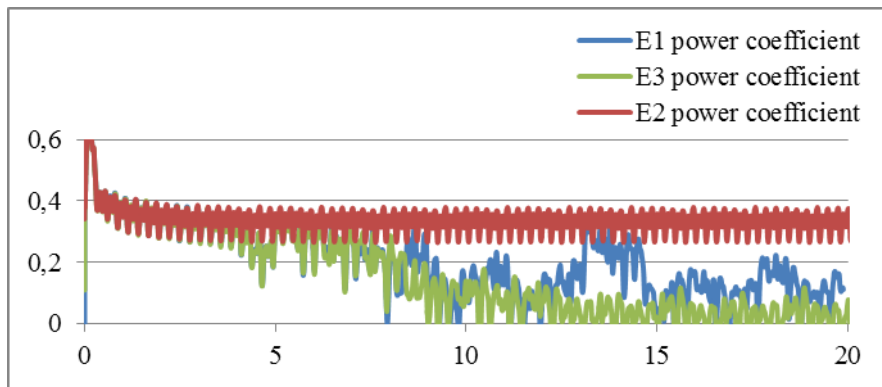


Figure 16. power coefficient with time – case L0-36 – $d'=15*D$

The calculations for cases L0-6, L0-12, L0-36 show that the performance of turbines just in the wake of the previous turbine decrease rapidly (figure 16). For example, for the case 0, 36, the power coefficient of the first turbine is 0.33, of the second 0.14 and of the third 0.14.

The present study shows that more the spacing turbine distance in the crosswind direction is small, better are the power coefficients. But the spacing turbine distance in the downwind direction has to be greater in order to keep a reasonable coefficient.

A first estimation of power density leads to an approximate value between 3 and 5 Wm^{-2} which is closer to HAWTs than VAWTs [6].

5 CONCLUSIONS

Modern wind farms of HAWTs require significant land resources to separate each wind turbine from the adjacent turbine wakes. This constraint limits the amount of power that can be extracted from a given wind farm footprint.

The use of a small VAWT with relative rotating blades was investigated in order to achieve medium power output per unit land area. Whereas modern wind farms consisting of HAWTs produce 2–3 W of power per square meter of land area, these calculations indicate that power densities are an order of magnitude equal or just greater. The results suggest an alternative approach to wind farming that has the potential to concurrently reduce the cost, size, and environmental impacts of wind farms. The present turbine will be used in urban configurations.

A short-cut model suitable for the best performance of the overall wind park can be drawn. The turbine grid can't be a uniform one. Each individual machine is equally placed between its neighbours in triangular configurations.

REFERENCES

- [1] Abbott, I. H., Von Doenhof, A. E. (1949), *Theory of wing sections*, Mc Graw Hill Book, ISBN 486-60586-8
- [2] Bayeul-Lainé A.C., Bois G. (2010), « Unsteady simulation of flow in micro vertical axis wind turbine », *Proceedings of 21st International Symposium on Transport Phenomena, Kaohsiung City Taiwan, 02-05 november*.
- [3] Bayeul-Lainé, A. C., Dockter, A., Bois, G., Simonet, S. (2011) , “Numerical simulation in vertical wind axis turbine with pitch controlled blades”, *IC-EpsMsO, 4th , Athens, Greece, 6-9 July, pp 429-436*, ISBN 978-960-98941-7-3
- [4] Cooper P., Kennedy O. (2005), “Development and analysis of a novel Vertical Axis Wind Turbine”, http://www.datataker.com/public_domain/PD71%20Development%20and%20analysis%20of%20a%20novel%20vertical%20axis%20wind%20turbine.pdf
- [5] Cooper P. (2010), *Wind Power Generation and wind Turbine Design*, WIT Press, chapter 8, ISBN 978-1-84564-205-1
- [6] Dabiri, J. O. (2011), “Potential order of magnitude enhancement of wind farm power density via counter-rotating vertical-axis wind turbine arrays”, *J. renewable Sustainable Energy* 3,043104, <http://dx.doi.org/10.1063/1.3608170>
- [7] Dieudonné P.A.M. (2006), « Eolienne à voilure tournante à fort potentiel énergétique », *Demande de brevet d'invention FR 2 899 286 A1, brevet INPI 0602890, 03 avril*
- [8] Hau, E. (2000), *Wind turbines*, Springer, Germany
- [9] Leconte, P., Rapin, M., Szechenyi, E. (2001), *Eoliennes*, Techniques de l'ingénieur BM 4 640, pp 1-24
- [10] Martin J. (1987), *Energies éoliennes*, Techniques de l'ingénieur B 8 585, pp 1-21
- [11] Menter, F. R. and Kuntz, M. (2002), *Adaptation of Eddy Viscosity Turbulence Models to Unsteady Separated Flows Behind Vehicles*, in *The Aerodynamics of Heavy Vehicles: Trucks, Buses and Trains*, Springer, Asilomar, CA.
- [12] Pawsey, N.C.K., (2002), *Development and evaluation of passive variable-pitch vertical axis wind turbines*, PhD Thesis, Univ. New South Wales, Australia